

RSC Advances



This is an *Accepted Manuscript*, which has been through the Royal Society of Chemistry peer review process and has been accepted for publication.

Accepted Manuscripts are published online shortly after acceptance, before technical editing, formatting and proof reading. Using this free service, authors can make their results available to the community, in citable form, before we publish the edited article. This *Accepted Manuscript* will be replaced by the edited, formatted and paginated article as soon as this is available.

You can find more information about *Accepted Manuscripts* in the [Information for Authors](#).

Please note that technical editing may introduce minor changes to the text and/or graphics, which may alter content. The journal's standard [Terms & Conditions](#) and the [Ethical guidelines](#) still apply. In no event shall the Royal Society of Chemistry be held responsible for any errors or omissions in this *Accepted Manuscript* or any consequences arising from the use of any information it contains.

COMMUNICATION

Phosphate Enriched Polyoxometalate Based Ionic Salts for Proton Conduction

Cite this: DOI: 10.1039/x0xx00000x

Chandan Dey,* Tanay Kundu, Harshitha Barike Aiyappa, and Rahul Banerjee*

Received 00th January 2012,

Accepted 00th January 2012

DOI: 10.1039/x0xx00000x

www.rsc.org/

A series of $[\text{NiMo}_{12}\text{O}_{30}(\text{PO}_4)_8]^{12-}$ POM anion and organic cation based ionic composites have been prepared in hydrothermal condition. The ionic composite with protonated ethylene diamine molecules have been tested for proton conductivity.

Solid state proton conduction¹ has caught recent attention owing to its advantages over the liquid counterpart *viz.*, safer, easy design, high shock resistance, wide electrochemical stability, etc; thereby augmenting their potential application in fuel cells, batteries and chemical sensors. Proton conducting materials play a crucial role in determining the performance of proton exchange membrane fuel cells (PEFMC's),² a promising means for renewable energy conversion. Till date, Nafion[®] is used as a standard proton conductor for low temperature fuel cell operation (<80°C) with proton conductivity up to 0.1 S/cm at requisite high levels of hydration.³ Apart from that, numerous metal oxides like MgCrO_4 - TiO_2 , ZrO_2 - MgO , $\text{Ba}_{0.5}\text{Sr}_{0.5}\text{TiO}_3$, TiO_2 - $\text{K}_2\text{Ti}_6\text{O}_{13}$, $\text{HZrP}_3\text{O}_{12}$ oxides⁴ are also tried as solid electrolytes for their proton conducting property at humidification condition. Recently, the nanocomposite membranes consisting of hydrophilic inorganic nanoparticles embedded polyelectrolytes have been in the limelight due to their proton conducting ability at high temperature.⁵ In addition, organic sulfonic and phosphonic acid functionalized mesoporous silica and zeolite are also rectified for proton conduction.⁶

Solid organic-inorganic hybrid materials with tunable porosity have been exploited for catalysis, selective sorption, ion exchange and ion conduction by the virtue of their tunable porosity.⁷ Polyoxometalates (POMs),⁸ composite of transition metal (Mo, W, V, etc.) oxide are highly thermal stable and hydrophilic in nature. These aforementioned facts encourage us to design phosphate decorated POM based hybrid materials for proton conduction.

Physical/Materials Chemistry Division, CSIR-National Chemical Laboratory, Dr. Homi Bhabha Road, Pune 411008, India; Tel: +912025902535; E-mail: ck.dey@ncl.res.in, r.banerjee@ncl.res.in

† Electronic Supplementary Information (ESI) available: Experimental procedures, crystallographic data (CIF) and additional supporting data. See DOI: 10.1039/b000000x/

Although POMs have desired functionality to be good proton conducting material, but so far report of POM based proton conducting materials are very few.⁹ Designing a POM based three dimensional hybrid materials with porous hydrophilic channel is challenging. Till date five different types of POM based composites, classified as (i) POM incorporated inside perfluorinated sulfonic acid polymer, (ii) POM immobilized in silica material via sol-gel method,

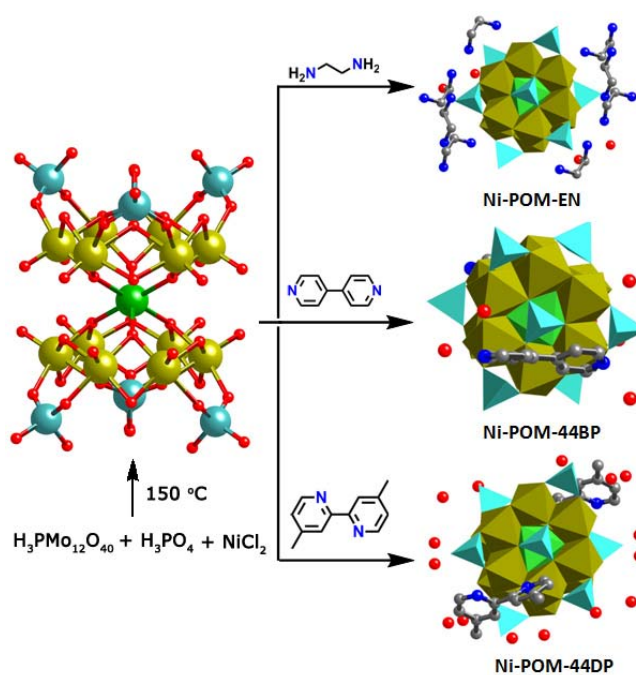


Figure 1: The constituent anion and cations to form ionic composites. The organic molecules get protonated in the reaction medium to form counter cations. In $[\text{NiMo}_{12}\text{O}_{30}(\text{PO}_4)_8]^{12-}$ anion yellow polyhedra represents MoO_6 units, green polyhedra represents NiO_6 units and cyan polyhedra represents PO_4 units; Red: O, Blue: N, Grey: C. Hydrogen atoms are omitted for clarity.

(iii) POM casted in inert polymer matrix, (iv) POM directly attached to polymer through functionalization, (v) POM based metal organic materials, have been tested for proton conductivity.¹⁰ Herein, we have synthesized POM anion and organic cations based ionic hybrid composites for proton conduction. To design such materials we have selected $[\text{NiMo}_{12}\text{O}_{30}(\text{PO}_4)_8]^{n-}$ POM anion¹¹ and ethylene-diamine (EN) / 4,4'-bipyridine (44BP) / 4,4'-dimethyl 2,2'-bipyridine (44DP), which eventually gets protonated in the reaction medium to form POM anion and organic cation based ionic composites (figure 1).

The development of metal oxide chemistry is reliant on the production of new architecture possessing unique structures and properties, although the production of such compounds by routine design remains elusive till date. Different synthetic methods, like hydrothermal synthesis, solvothermal synthesis, ionothermal synthesis, microwave synthesis, etc. have already been used to synthesize POM based material, but hydrothermal synthesis is most efficient method used so far.¹² The $[\text{NiMo}_{12}\text{O}_{30}(\text{PO}_4)_8]^{n-}$ POM can be considered as dimer of $\text{Mo}_6\text{O}_{15}(\text{PO}_4)_4$ (figure 2a) connected via M (where M= Ni, Co, Cr etc). This POM contains eight of phosphate functionality per unit, which could be the potential candidates for catalysis in its inter-crystalline region. The most of the POM of this type are classified as reduced molybdenum cluster because few of the molybdenum of the cluster are in V oxidation state whereas rest are in regular VI oxidation state.¹³ To synthesize such compound metallic molybdenum(0) was used with molybdenum(VI) precursor in the reaction medium.¹⁴ There are reports of synthesis of reduced POM prepared from Mo(VI) precursor without Mo(0) source.¹⁵ However, we have used only molybdenum(VI) compound as a starting material during synthesis. Hydrothermal method was used to synthesize all the compounds (150 °C for 96 hours). The reaction conditions almost remain same for all the synthesis reported in the work, except the change in the organic moiety for individual ionic composite. All three ionic crystal reported in this paper was synthesised in hydrothermal condition using the mixture of 20 wt% solution of phosphomolybdic acid in ethanol (1 mL), 85% H_3PO_4 (0.5 mL), $\text{NiCl}_2 \cdot 6\text{H}_2\text{O}$ (0.21 mmol) and organic counterpart (for Ni-POM-EN, ethylene diamine molecules; for Ni-POM-44BP, 4,4'-bipyridine; for Ni-POM-44DP, 4,4'-dimethyl 2,2'-bipyridine.) in water.

The asymmetric unit of Ni-POM-EN crystal structure (triclinic, space group: *P*-1) contains half of $[\text{NiMo}_{12}\text{O}_{30}(\text{PO}_4)_8]^{n-}$ POM unit, two and half dication of ethylene diamine and four water molecules (figure 2b). The charge of the material is balanced by protonation of ethylene diamine molecules. The protons were identified and located crystallographically inside crystal structure. In the system two of ethylene diamine molecules are in *anti* form and one is in *gauche* form. The $[\text{NiMo}_{12}\text{O}_{30}(\text{PO}_4)_8]^{n-}$ anion can be described as a dimer of two $\text{Mo}_6\text{O}_{15}(\text{PO}_4)_4$ hexanuclear rings, connected via one Ni(II) octahedra. Each monomer ring, $\text{Mo}_6\text{O}_{15}(\text{PO}_4)_4$ consists of six edge shared MoO_6 polyhedra units. Inside the ring the distance between two opposite Mo atom is 6.081 Å. The periphery of the ring is decorated by three tetrahedral phosphate [The average P-O distance ranges from 1.512(7) to 1.568(7) Å] groups at an alternate position in-between two MoO_6 units. One more phosphate group is exposed from the centre of the ring connecting three $[\text{MoO}_6]_2$ units in a ring (figure 2a). In the cluster the average Mo-O bond distance lies in-between 1.668(7)-2.297(6) Å and the average Ni-O bond distance is 2.145 Å. The POMs are arranged in crystallographic *ac*-plane to form a two dimensional layers arrangement. The

layers are stack on top of each other through crystallographic *b*-axis. Free solvent molecules and ethylene diamine molecules

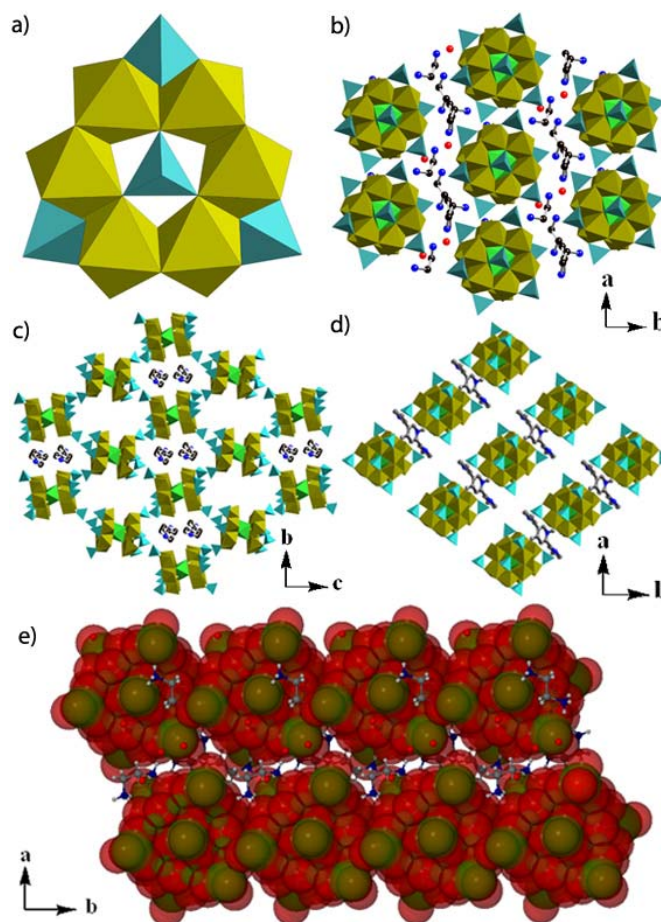


Figure 2: (a) Monomeric unit, $\text{Mo}_6\text{O}_{15}(\text{PO}_4)_4$ which connected via Ni(II) to form $[\text{NiMo}_{12}\text{O}_{30}(\text{PO}_4)_8]^{n-}$ in crystal structure. Crystal structure of (b) Ni-POM-EN, (c) Ni-POM-44BP, (d) Ni-POM-44DP. POM units are represented in polyhedral model and whereas counter cation are represented in ball-stick model. Solvent molecules for Ni-POM-44BP and Ni-POM-44DP have been removed from clarity. Cyan: PO_4 , Yellowish green: MoO_6 , Green: NiO_6 , Blue: N, Red: O. (e) Space fill model of Ni-POM-EN showing the floating cationic counterpart and solvent molecules (ball-stick) in-between two layers which create proton conducting pathway.

are floated in-between layers of POMs which act as proton conducting pathway inside the structure (figure 2e). The ethylene diamine and water molecules are hydrogen bonded to oxygen of POM units. The average hydrogen bonding distances between protonated ethylene diamine molecules and POM units are in the range of 2.638–3.053 Å. Whereas the average hydrogen bonding distance among water molecules and POM unit are in the range of 2.288–2.900 Å. There is already a report of $[\text{NiMo}_{12}\text{O}_{30}(\text{PO}_4)_8]^{n-}$ anion and ethylene diamine based ionic composite which also crystallizes in *P*-1 space group but unit cell parameters [$a = 13.22$ Å, $b = 21.79$ Å, $c = 15.59$ Å. $\alpha = 90^\circ$, $\beta = 110.06^\circ$, $\gamma = 90.00^\circ$] are different from the crystal reported in this paper.¹⁶

Ni-POM-44BP crystallizes in monoclinic crystal system (space group: $P2_1/c$). The asymmetric unit consists of one

$[\text{NiMo}_{12}\text{O}_{30}(\text{PO}_4)_8]^{12-}$ POM anion, one 4,4'-bipyridine molecule and eight water molecules (figure 2c). The solvent (water) and 4,4'-bipyridine molecules are protonated to balance the charge. The 4,4'-bipyridine molecules and POM anions are alternatively arranged in crystallographic *ac*-plane to form two dimensional sheets. These sheets are stack on top of each other through crystallographic *b*-axis with inter layer distance of ~ 3.601 Å. In-between two parallel sheets protonated water molecules are laying. The water molecules are hydrogen bonded with other water molecules and POM cluster (closest hydrogen bonding distance: 2.317 Å), which help to hold the three dimensional arrangement. The reported crystal structure with 4,4'-bipyridine molecule and same anion crystallizes in *Pccn* space group with unit cell parameter; $a = 27.74$ Å, $b = 16.15$ Å, $c = 22.82$ Å and $\alpha = \beta = \gamma = 90^\circ$.¹⁷ The asymmetric unit of Ni-POM-44DP crystal structure (triclinic, space group: *P*-1) contains half of $[\text{NiMo}_{12}\text{O}_{30}(\text{PO}_4)_8]^{12-}$ POM unit, one 4,4'-dimethyl 2,2'-pyridyl and seven water molecules (figure 2d). Each POM unit is surrounded by six 4,4'-dimethyl 2,2'-pyridyl molecules. The 'N' atoms from each 4,4'-dimethyl 2,2'-pyridyl molecule are hydrogen bonded to 'O' atoms of POM [$\text{N}-\text{O}$] distance: 2.609(6) Å and 2.690(7) Å respectively]. This unit repeats in the crystallographic *ac*-plane to form two dimensional sheets. These sheets are stack on top of each other through crystallographic *b*-axis with an inter layer distance of ~ 3.664 Å. In a sheet the distance between two closest POMs is 13.743 Å along crystallographic *b*-axis, whereas the distance is 12.891 Å along *a*-axis.

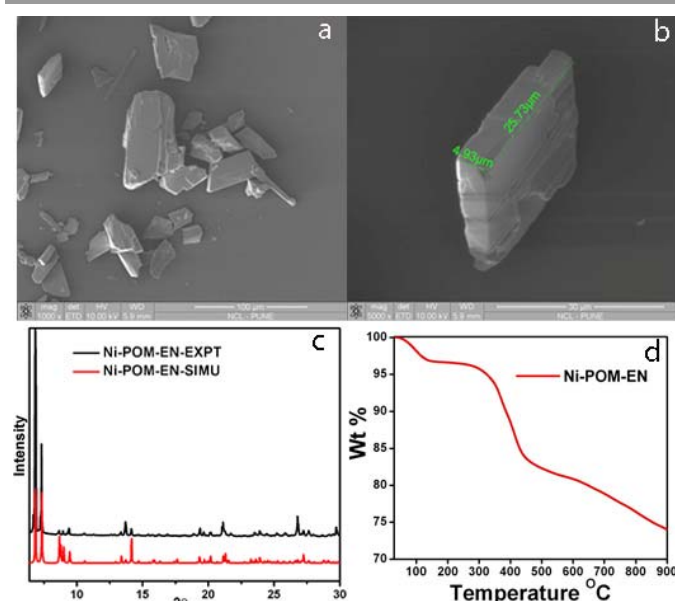


Figure 3: (a) SEM image of as-synthesized Ni-POM-EN showing bulk morphology. (b) SEM image of rectangular shaped single crystal of Ni-POM-EN. (c) Simulated (bottom) and experimental (top) PXRD pattern of Ni-POM-EN. (d) Thermal Gravimetric Analysis curve for Ni-POM-EN.

The scanning electron microscopy (SEM) images of as-synthesized Ni-POM-EN disclose rectangular shape morphology of the bulk material (figure 3a). The crystals are having $\sim 25\mu\text{m}$ length and $\sim 5\mu\text{m}$ width in average (figure 3b). The PXRD pattern of as-synthesized compound matches quite well with the simulated pattern which proves phase purity of bulk Ni-POM-EN (figure 3c). The thermal stability of Ni-

POM-EN was examined using thermo gravimetric analysis (TGA) data, collected in the temperature range of 30–900 °C. The compound is stable upto 350 °C, beyond this temperature it starts decomposing. The $\sim 3\%$ loss of weight around 100 °C is duo to removal of non-coordinated water molecules from the structure (figure 3d). The Ni-POM-EN displays characteristic IR frequencies for $[\text{NiMo}_{12}\text{O}_{30}(\text{PO}_4)_8]^{12-}$ POM units at 1117($\nu_{\text{asym}}\text{P}-\text{O}_a$), 998($\nu_{\text{asym}}\text{P}-\text{O}_b$), 897($\nu_{\text{asym}}\text{Mo}=\text{O}$), 819 ($\nu_{\text{asym}}\text{Mo}-\text{O}_a$), 725($\nu_{\text{asym}}\text{Mo}-\text{O}_b$) and 668 ($\nu_{\text{asym}}\text{Mo}-\text{O}_c$) cm^{-1} (figure S9 in ESI). PRXD of Ni-POM-EN was also recorded after proton conductivity measurement. The PXRD pattern of the sample obtained after proton conductivity measurement shows a different crystalline phase, whereas heating at 60 °C causes the regeneration of parent phase. Heating of the sample at 180 °C (Ni-POM-EN-180) generates a completely new phase due to the removal of all solvent molecules (figure S18 in ESI). The IR spectroscopic analysis of sample, Ni-POM-EN-180 shows shift from 897 to 945 cm^{-1} and 989 to 1005 cm^{-1} . The shift could be due to the removal of hydrogen bonded water molecules from the structure (figure S10 in ESI). We could not able to make Ni-POM-44BP and Ni-POM-44DP in bulk as a pure form due to simultaneous formation of different phases. However, the analysis of Ni-POM-44BP and Ni-POM-44DP crystal structures suggest that both the compound in pure phase could be used as proton conducting material.

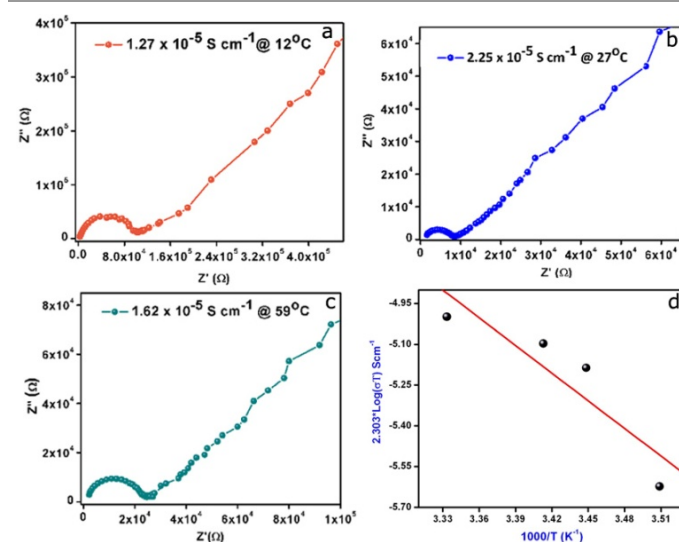


Figure 4: Nyquist plot of proton conduction for Ni-POM-EN with 98% RH condition (a) at 12 °C, (b) at 27 °C and (c) at 59 °C. (d) Arrhenius plot of proton conductivity of Ni-POM-EN. Least square fitting is shown as a straight line.

POM based composite materials have drawn current research attention for proton conductivity in fuel cell application. CsHSO_4 and $\text{H}_3\text{PW}_{12}\text{O}_{40}\cdot 6\text{H}_2\text{O}$ composite prepared by mechanical milling have shown proton conductivity $3.3 \times 10^{-3} \text{ Scm}^{-1}$ at 100 °C.^{9a} Proton conducting gel, prepared by encapsulating heteropolyacids within Poly(methyl methacrylate) matrix showed proton conductivity in range of temperature, -60 °C to 90 °C ($5 \times 10^{-4} \text{ Scm}^{-1}$ and $8 \times 10^{-4} \text{ Scm}^{-1}$ respectively).^{9d} POM embedded glass composite membrane prepared by sol-gel method exhibit proton conductivity, $1.01 \times 10^{-1} \text{ Scm}^{-1}$ with 85% relative humidity (RH) at 85 °C.¹⁸ In our earlier work, we have designed POM based metal organic material which display proton conductivity

of $1.0 \times 10^{-5} \text{ Scm}^{-1}$ at 34 °C with 98% relative humidity (RH).¹⁹ In this work we have experimented proton conduction on POM based ionic composite. Electrochemical impedance measurements were carried out to determine the proton conductivity of the composite at different temperatures. The Nyquist plots obtained at each temperature were used to determine the proton conductivity of Ni-POM-EN using the relation, $\sigma = L/(S \times R)$ equation, where R is the resistance, L is the width, and S is the area of the sample plate. The conductivity value recorded at room temperature (27 °C) and 98% relative humidity (RH) is $2.25 \times 10^{-5} \text{ Scm}^{-1}$, highest for Ni-POM-EN in the temperature range of 12 °C to 59 °C (figure 4b). We have observed relatively low proton conductivity value at high temperature as well as low temperature compare to room temperature value. The proton conductivity value measured at 12 °C, 17 °C, 20 °C, 39 °C and 59 °C (with 98 % RH) are 1.27×10^{-5} , 1.93×10^{-5} , 2.09×10^{-5} , $1.69 \times 10^{-5} \text{ Scm}^{-1}$ respectively (Section S6 in ESI). The activation energy calculated using Arrhenius equation was found to be 0.29 eV (figure 4d), indicative of an efficient Grotthuss mechanism for proton conduction.

In conclusion, we have synthesized a series of organic cations and polyoxometalate based hybrid ionic composites. The presence of phosphate functionality and hydrogen bonded water imparts temperature dependent proton conducting ability to Ni-POM-EN. The synthetic method reported here could further be adapted for directional design and synthesis of new polyoxometalate based ionic architectures for sorption, conductivity, magnetism, etc. The presence of phosphate functionality of this particular polyoxometalate could facilitate catalytic activity in the intra crystalline region.

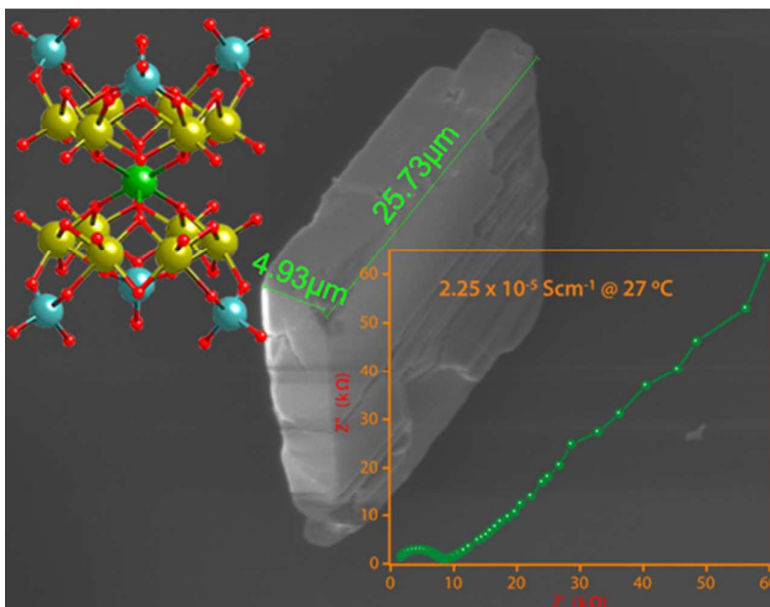
Acknowledgements

CD, TK acknowledge CSIR, New Delhi, India and HBA acknowledges UGC for fellowship support. R.B. acknowledges grant GAP-304326 from Department of Science & Technology (DST) and CSIR's Five Year Plan (CSC0122 and CSC0102) for funding. We thank Dr. Sreekumar Kurungot for helping us to measure proton conductivity of the material.

References

- (a) K. -D. Kreuer, *Chem. Mater.* 1996, **8**, 610. (b) H. Wang, X. Xu, N. M. Johnson, N. K. R. Dandala and H.-F. Ji, *Angew. Chem. Int. Ed.* 2011, **50**, 12538.
- (a) Y. -J. Wang, D. P. Wilkinson and J. Zhang, *Chem. Rev.* 2011, **111**, 7625. (b) K. -D. Kreuer, S. J. Paddison, E. Spohr and M. Schuster, *Chem. Rev.* 2004, **104**, 4637.
- K. A. Mauritz and R. B. Moore, *Chem. Rev.* 2004, **104**, 4535.
- (a) T. Uma and M. Nogami, *Chem. Mater.* 2007, **19**, 3604. (b) S. Fengf and M. Greenblatt, *Chem. Mater.* 1993, **5**, 1277. (c) Y. Yamazaki, R. Hernandez-Sanchez and S. M. Haile, *Chem. Mater.* 2009, **21**, 2755. (d) J. C. McKeen, Y. S. Yan and M. E. Davis, *Chem. Mater.* 2008, **20**, 5122. (e) F. M. Vichi, M. I. Tejedor-Tejedor and M. A. Anderson, *Chem. Mater.* 2000, **12**, 1762. (f) J. F. Shin, K. Joubel, D. C. Apperley and P. R. Slater, *Dalton Trans.* 2012, **41**, 261. (g) M. Nogami, R. Nagao, C. Wong, T. Kasuga and T. Hayakawa, *J. Phys. Chem. B.* 1999, **103**, 9468.
- (a) J. J. Smith and I. Zharov, *Chem. Mater.* 2009, **21**, 2013. (b) X. Wei and M. Z. Yates, *Chem. Mater.* 2012, **24**, 1738.
- (a) J. C. McKeen, Y. S. Yan and M. E. Davis, *Chem. Mater.* 2008, **20**, 3791. (b) J. M. Taylor, R. K. Mah, I. L. Moudrakovski, C. I. Ratcliffe, R. Vaidhyanathan, and G. K. H. Shimizu, *J. Am. Chem. Soc.* 2010, **132**, 14055. (c) J. C. McKeen, Yushan S. Yan and M. E. Davis, *Chem. Mater.* 2008, **20**, 5122.
- (a) R. Banerjee, A. Phan, B. Wang, C. Knobler, H. Furukawa, M. O'Keeffe and O. M. Yaghi, *Science*, 2008, **319**, 939. (b) S. C. Sahoo, T. Kundu and R. Banerjee, *J. Am. Chem. Soc.* 2011, **133**, 17950. (c) C. Dey, R. Das, P. Pachfule, P. Poddar, R. Banerjee, *Cryst. Growth Des.* 2011, **11**, 139. (d) S. Chandra, T. Kundu, S. Kandambeth, R. BabaRao, Y. Marathe, S. M. Kunjir, and R. Banerjee, *J. Am. Chem. Soc.* 2014, **136**, 6570. (e) A. Mallick, T. Kundu and R. Banerjee, *Chem. Commun.* 2012, **48**, 8829. (f) T. Panda, T. Kundu and R. Banerjee, *Chem. Commun.* 2013, **49**, 6197. (g) C. Dey and R. Banerjee, *Chem. Commun.* 2013, **49**, 6617. (h) T. Panda, T. Kundu and R. Banerjee, *Chem. Commun.* 2012, **48**, 5464. (i) S. Sen, N. N. Nair, T. Yamada, H. Kitagawa, and P. K. Bharadwaj, *J. Am. Chem. Soc.* 2012, **134**, 19432.
- (a) D. -L. Long, R. Tsunashima, and L. Cronin, *Angew. Chem. Int. Ed.* 2010, **49**, 1736. (b) R. Neumann and M. Dahan, *Nature*. 1997, **388**, 353. (c) N. Mizuno and M. Misono, *Chem. Rev.* 1998, **98**, 199. (d) C. P. Pradeep, D. -L. Long, C. Streb and L. Cronin, *J. Am. Chem. Soc.* 2008, **130**, 14946.
- (a) Y. Daiko, S. Hayashi and A. Matsuda, *Chem. Mater.* 2010, **22**, 3418. (b) T. Uma and M. Nogami, *Chem. Mater.* 2007, **19**, 3604. (c) X. Tong, X. Wu, Q. Wu, W. Zhu, F. Cao, W. Yan, *Dalton Trans.* 2012, **41**, 9893. (d) K. Checkiewicz, G. Zukowska and W. Wiczorek, *Chem. Mater.* 2001, **13**, 379. (e) T. Uma and M. Nogami, *Chem. Mater.* 2007, **19**, 3604.
- S. Sachdeva, J. A. Turner, J. L. Horan, A. M. Herring, *Struct. Bond.* 2011, **141**, 115.
- (a) C. Streb, D. -L. Long and L. Cronin, *Chem. Commun.* 2007, 471. (b) L. A. Mudit, R. C. Haushalter, *Inorg. Chem.* 1992, **31**, 3050. (c) W. -J. Chang, Y.-C. Jiang, S.-L. Wang, K. -H. Lii, *Inorg. Chem.* 2006, **45**, 6586. (d) Y.-S. Zhou, L. -J. Zhang, H. -K. Fun, J. -L. Zuo, I. A. Razak, S. Chantrapromma and X. -Z. You, *New J. Chem.* 2001, **25**, 1342. (e) A. Guesdon, M. M. Borel, A. Leclaire and B. Raveau, *Chem. Eur. J.* 1997, **3**, 1797.
- (a) C. Dey, R. Das, P. Poddar and R. Banerjee, *Cryst. Growth Des.* 2012, **12**, 12. (b) K. E. Knope, and C. L. Cahill, *Inorg. Chem.* 2007, **46**, 6607.
- C. Baffert, J. F. Boas, A. M. Bond, P. Kçgerler, D. -L. Long, J. R. Pilbrow, and L. Cronin, *Chem. Eur. J.* 2006, **12**, 8472.
- A. Leclaire, C. Biot, H. Rebbah, M. M. Borela and B. Raveau, *J. Mater. Chem.*, 1998, **8**, 439.
- S. Wang, E. Wang, Y. Hou, Y. Li, Li Wang, Mei Yuan and Changwen Hu, *Transit. Met. Chem.* 2003, **28**, 616.
- L. Xu, Y. Sun, E. Wang, E. Shen, Z. Liu, C. Hu, Y. Xing, Y. Lin and H. Jia, *J. Solid. State. Chem.* 1999, **146**, 533.
- W. -J. Chang, Y. -C. Jiang, S. -L. Wang, and K. -H. Lii, *Inorg. Chem.* 2006, **45**, 6586.
- M. Yamada, D. Li, I. Honma, and H. Zhou, *J. Am. Chem. Soc.* 2005, **127**, 13092.
- C. Dey, T. Kundu and R. Banerjee. *Chem. Commun.* 2012, **48**, 266.

TABLE OF CONTENT GRAPHIC



A rarely observed phosphate enriched POM anion, $[\text{NiMo}_{12}\text{O}_{30}(\text{PO}_4)_8]^{n-}$ was synthesized and crystallized with protonated ethylene diamine in one-pot reaction. The composite was tested for proton conductivity measurement.